[6]Gaffney, R. L., Salas, M. D., and Hassan, H. A., "An Abbreviated Reynolds Stress Turbulence Model for Airfoil Flows," AIAA Paper 90-1468, June 1990.

[7]Patel, V. C., Rodi, W., and Scheuerer, G., "Turbulence Models for Near-Wall and Low Reynolds Number Flows: A Review," *AIAA Journal*, Vol. 23, No. 9, 1985, pp. 1308–1319.

[8]Speziale, C. G., Abid, R., and Anderson, E. C., "Critical Evaluation of Two-Equation Models for Near-Wall Turbulence," *AIAA Journal*, Vol. 30, No. 2, 1992, pp. 324–331.

[9]Wilcox, D. C., *Turbulence Modeling for CFD*, DCW Industries, La Cañada, CA, 1993.

[10]Robinson, D. F., and Hassan, H. A., "A Two-Equation Turbulence Closure Model for Wall Bounded and Free Shear Flows," AIAA Paper 96-2057, June 1996.

[11]Mansour, N. N., Kim, J., and Moin, P., "Reynolds Stress and Dissipation Rate Budgets in Turbulent Shear Flows," *Journal of Fluid Mechanics*, Vol. 194, Pt. 1, 1988, pp. 15–44.

[12]Laufer, J., "Investigation of Turbulent Shear Flow in a Two-Dimensional Channel," NACA Rept. 1053, 1951.

[13]Pot, P. J., "Measurement in a Two-Dimensional Wake and in a Two-Dimensional Wake Merging into a Boundary Layer," NLR, TR-79063 U, The Netherlands, 1979.

[14]Weygandt, J. H., and Mehta, R. D., "Asymptotic Behavior of a Flat Plate Wake," NASA CR-185917, 1989.

[15]Thibert, J. J., Granjacques, M., and Ohman, L. H., "Experimental Data Base for Computer Program Assessment, NACA 0012 Airfoil," AGARD Advisory Rept. No. 138, May 1979.

D. S. McRae
*Associate Editor*

# Alternative to the $e^n$ Method for Determining Onset of Transition

E. W. Warren* and H. A. Hassan†
*North Carolina State University, Raleigh, North Carolina 27695-7910*

## Introduction

THE process of transition from laminar to turbulent flow remains one of the most important unsolved problems in fluid mechanics and aerodynamics. Transitional flows are characterized by increased skin friction and heat transfer, and the accurate determination of heating rates and drag critically depends on the ability to predict the onset and extent of transition. However, no mathematical model exists that can accurately predict the location of transition under a wide range of conditions. Design engineers resort to methods that are based on either empirical correlations or linear stability theory.

The $e^n$ method is currently the method of choice for determining transition onset. The method is based on linear stability theory and generally requires the following steps.

1) Mean flow must be precalculated at a large number of streamwise locations along the body of interest.

2) At each streamwise station, a local linear stability analysis is performed. By assumptions of the linear theory, the unsteady disturbances are decomposed into separate normal modes of different frequency. The stability equations are solved for the spatial amplification rate of each unstable frequency.

3) An amplitude ratio for each frequency is then calculated by integrating the spatial amplification rate in the streamwise direction on the body, i.e.,

$$\ln\left(\frac{A}{A_0}\right) = \int_{x_0}^{x} \alpha_i \,\mathrm{d}x \tag{1}$$

4) The $n$ factor is then determined by taking the maximum of the just calculated quantity at each streamwise location.

The major problem with the $e^n$ method is that the $n$ factor does not represent the amplitude of a disturbance in the boundary layer but rather an amplification factor from an unknown amplitude $A_0$. The amplitude $A_0$ represents the amplitude of a disturbance of specified frequency at its neutral stability point. Its value is related to the external disturbance environment through some generally unknown receptivity process. As a consequence, the value of $n$ that determines transition onset must be correlated to available experimental data.[1] Additionally, the $e^n$ method requires the use of several computational tools such as a boundary-layer or Navier–Stokes flow solver to calculate the mean flow and the linear stability solver to determine the amplification rates.[2] Methods based on the nonlinear parabolized stability equations[3] (PSE) are being used to determine transition onset but they have not received the wide acceptance enjoyed by the $e^n$ method. Methods based on the PSE also require precalculation of the mean flow and specification of initial conditions such as frequency and disturbance eigenfunctions. Methods based on linear stability theory only provide an estimation of the location of transition and can provide no information about the subsequent transitional and turbulent flow.

In this work, a different approach has been developed, which does not require precalculation of the mean flow or the specification of frequencies. It determines the transition onset and calculates the laminar, transitional, and turbulent regions in a single computation. The approach employs a two-equation model similar to that employed in turbulent calculations. It is based on the premise that, if a flow quantity can be written as the sum of a mean and a fluctuating quantity, then the exact equations that govern the fluctuations and their averages are identical irrespective of the nature of the oscillations, i.e., laminar, transitional, or turbulent. Moreover, if it is possible to model the equations governing the mean energy of the fluctuations and their rate of decay (or other equations) in such a way that one does not appeal to their nature, then the resulting model equations will be formally identical. However, the parameters that appear in the modeled equations will depend on the nature of the fluctuations. As an illustration, let us assume that we employ a Boussinesq approximation to model the stresses resulting from the fluctuations, i.e.,

$$\tau_{ij} = -\rho\overline{u_i'u_j'} = \mu_t\left(2S_{ij} - \frac{2}{3}\delta_{ij}\frac{\partial U_m}{\partial x_m}\right) - \frac{2}{3}\rho k\delta_{ij} \tag{2}$$

where

$$S_{ij} = \frac{1}{2}\left(\frac{\partial U_i}{\partial x_j} + \frac{\partial U_j}{\partial x_i}\right), \qquad k = \frac{1}{2}\overline{u_i'u_i'}$$

and where $\rho$ is the density, $U_i$ is the mean velocity, $\delta_{ij}$ is the Kronecker delta, and $\mu_t$ is the coefficient of viscosity brought about by the presence of fluctuations. The form indicated in Eq. (2) is used for all fluctuations, but the expressions for $\mu_t$ are quite different because the physics governing them is different.

The present approach is developed in conjunction with the $k$–$\zeta$ turbulence model of Robinson et al.[4] Details of the approach are given in Ref. 5. To explain its nature, the modeled $k$-equation is written as[5]

$$\frac{\mathrm{D}k}{\mathrm{D}t} = -\overline{u_i'u_j'}\frac{\partial U_i}{\partial x_j} - \frac{k}{\tau_k} + \frac{\partial}{\partial x_j}\left[\left(\frac{\nu}{3} + \frac{\nu_t}{\sigma_k}\right)\frac{\partial k}{\partial x_j}\right] \tag{3}$$

where $\nu_t = \mu_t/\rho$ and $\nu$ is the molecular kinematic viscosity. As may be seen from Eq. (3) and Refs. 5 and 6, to close the model one needs

Received Nov. 16, 1996; revision received Sept. 5, 1997; accepted for publication Sept. 10, 1997. 

*Research Assistant, Mechanical and Aerospace Engineering. Member AIAA.

†Professor, Mechanical and Aerospace Engineering. Associate Fellow, AIAA.

to specify $\nu_t$ and $\tau_k$, which is a representative decay time. Within the laminar region, these quantities will be determined based on results of linear stability theory.

For subsonic Mach numbers and regions where crossflow instability is unimportant, the dominant mode of instability is the first mode or the Tollmien–Schlichting (T–S) mode. For low-speed flows, the dominant disturbance frequency at breakdown is well predicted by the frequency of the first mode disturbance having the maximum amplification rate. Using the work of Obremski et al.,[7] Walker[8] showed that this frequency can be correlated by

$$\omega\nu/U_e^2 = 3.2Re_{\delta^*}^{-\frac{3}{2}} \tag{4}$$

where $U_e$ is the velocity at the edge of the boundary layer, $Re_{\delta^*}$ is the edge Reynolds number based on displacement thickness $\delta^*$, and $\omega$ is the frequency.

The eddy viscosity resulting from fluctuations in the laminar region can be modeled by

$$\nu_t = C_\mu k\tau_{\mu_\ell}, \qquad C_\mu = 0.09 \tag{5}$$

where $\tau_{\mu_\ell}$ is a viscosity timescale. Using the frequency of the dominant T–S disturbance, the viscosity timescale can be modeled in the laminar region as

$$\tau_{\mu_\ell} = a/\omega \tag{6}$$

where $a$ is a model constant. Within the laminar region, the representative decay time for the kinetic energy is modeled as

$$1/\tau_{k_\ell} = a(\nu_t/\nu)S, \qquad S^2 = S_{ij}S_{ij} \tag{7}$$

The quantities appropriate for turbulent flows, $\tau_{\mu_t}$ and $\tau_{k_t}$, are taken from Ref. 6. Quantities that are valid throughout the flowfield are obtained in terms of the quantities $\tau_{\mu_\ell}$, $\tau_{k_\ell}$, $\tau_{\mu_t}$, and $\tau_{k_t}$ and the intermittency $\Gamma$, which represents the fraction of time that the flow is turbulent. At a given point, the flow is laminar $(1-\Gamma)$ of the time and turbulent $\Gamma$ of the time. This allows the viscosity timescale to be written as a transitional viscosity timescale, i.e.,

$$\tau_\mu = (1-\Gamma)\tau_{\mu_\ell} + \tau_{\mu_t} \tag{8}$$

Similarly,

$$1/\tau_k = (1-\Gamma)\left(1/\tau_{k_\ell}\right) + \Gamma\left(1/\tau_{k_t}\right) \tag{9}$$

The intermittency $\Gamma$ is currently given by the Dhawan and Narasimha[9] expression

$$\Gamma(x) = 1 - \exp(-A\xi^2) \tag{10}$$

with

$$\xi = \frac{\max(x - x_t, 0)}{\lambda}, \qquad A = 0.412 \tag{11}$$

where $x_t$ denotes the transition point and $\lambda$ characterizes the extent of transition. For attached flows, an experimental correlation between $\lambda$ and $x_t$ is

$$Re_\lambda = 9.0Re_{x_t}^{0.75} \tag{12}$$

The transition point $x_t$ is determined as a part of the solution procedure and is the point that corresponds to the minimum skin friction.

The model constant $a$ is determined in the current work by comparing with the flat-plate experiments of Schubauer and Klebanoff[10] and Schubauer and Skramstad.[11] These classical experiments are well documented in the literature and cover a range of freestream turbulence intensities $Tu$. The constant is correlated as a function of the freestream intensity as

$$a = 0.0095 - 0.019Tu + 0.069(Tu)^2 \tag{13}$$

## Results

The present model was incorporated into the boundary-layer (BL) code of Harris and Blanchard[12] and the Navier–Stokes (NS) code of Robinson and Hassan.[6] The boundary conditions used in these calculations are those appropriate for any turbulence calculation. Further, grid convergence studies were conducted and the results are grid resolved. The BL calculations were carried out with approximately 100 points normal to the wall. Computations with the NS code for flat plates were carried out on a grid with 100 points in the streamwise direction and 50 points normal to the wall. Calculations for the airfoil cases were done on a grid with 256 points along the airfoil and 91 points normal to the wall.

The location of minimum skin friction is commonly taken as the onset of transition. In practice, it is very difficult to determine the minimum skin friction point in an evolving calculation. This can be due to either the transient nature of NS calculations or local oscillations in the skin friction itself, as seen in later airfoil results. To alleviate this problem, an alternate criterion was developed by comparing with the flat plate results. It was observed that the present method predicted the local skin-friction minimum at a location along the plate where the maximum $\nu_t/\nu \approx 9\%$. This criterion can be stated differently by noting that the turbulent Reynolds number $Re_T$ can be written in the laminar region $(\Gamma = 0)$ as

$$Re_T = (1/C_\mu)(\nu_t/\nu) \tag{14}$$

Written in this form, $Re_T$ can be considered a fluctuation Reynolds number instead of a turbulent Reynolds number. The location of transition onset $x_t$ is then determined as the minimum distance along the surface for which $Re_T \geq 1$.

Only limited results are presented here; additional results are available in Ref. 5. Figure 1 compares results from the present method with the skin-friction measurements of Schubauer and Klebanoff over a flat plate.[10] As is seen, both BL and NS codes well predict the transition onset and skin-friction distribution throughout the flowfield. To determine the validity of the correlation for the model constant, the airfoil experiments of Mateer et al.[13] are considered. They employed a supercritical airfoil over a range of angles of attack and Reynolds numbers. Figure 2 compares current predictions using both BL and NS codes and those using the $e^n$ method and the turbulence model of Menter[14] with experiment. The conditions of the experiment are Reynolds number of $2 \times 10^6$, a freestream Mach number of 0.2, an angle of attack of $-0.5$ deg, and freestream rms pressure and velocity disturbance levels of $0.02P_\infty$ and $0.005U_\infty$, respectively. As is seen in Fig. 2, the present model does a much better job than the $e^n$ method in predicting transition onset.

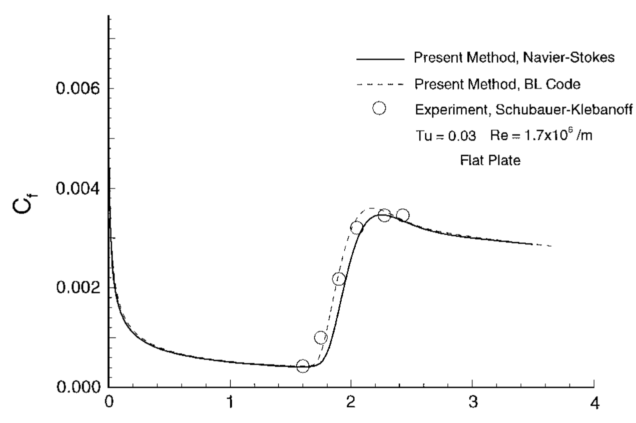


**Fig. 1 Comparison of present method with the experiment of Schubauer and Klebanoff,[10] $Re = 1.67 \times 10^6$/m, BL code.**

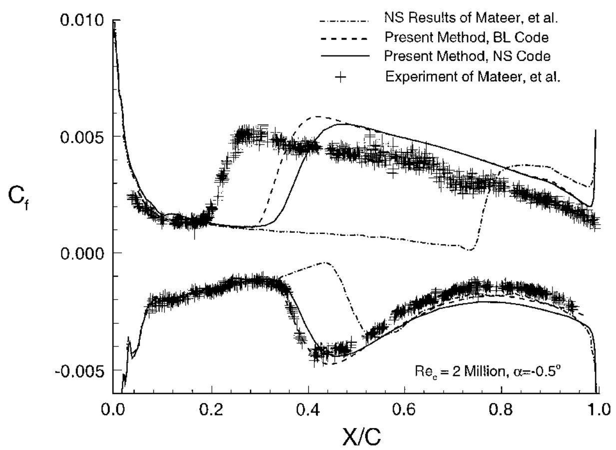


**Fig. 2 Comparison of present method and $e^n$ method with the airfoil experiment of Mateer et al.,[13] $Re_c = 2 \times 10^6$, $\alpha = -0.5$ deg.**

## Conclusion

In summary, the present model requires replacing $\nu_t$ and $\tau_k$ in any two-equation turbulence code by Eqs. (8) and (9) to calculate transition onset and the complete flowfield. Because of this, the present approach provides an inexpensive alternative to the $e^n$ method and methods based on the nonlinear PSE.

## Acknowledgments

This work is supported, in part, by NASA Grant NAG-1-244 from NASA Langley Research Center. Part of the computations were carried out at the North Carolina Supercomputing Center. The authors would like to acknowledge helpful discussions with Ndaona Chokani of North Carolina State University.

## References

[1]Mack, L. M., "Transition Prediction and Linear Stability Theory," AGARD CP-224, 1977, pp. 1-1–1-22.

[2]Saric, W. S., "Physical Description of Boundary Layer Transition: Experimental Evidence," AGARD Rept. 793, March 1993.

[3]Herbert, T., "Parabolized Stability Equations," AGARD Rept. 794, March 1993.

[4]Robinson, D. F., Harris, J. E., and Hassan, H. A., "Unified Turbulence Closure Model for Axisymmetric and Planar Free Shear Flows," *AIAA Journal*, Vol. 33, No. 12, 1995, pp. 2325–2331.

[5]Warren, E. S., and Hassan, H. A., "An Alternative to the $e^n$ Method for Determining Onset of Transition," AIAA Paper 97-0825, Jan. 1997.

[6]Robinson, D. F., and Hassan, H. A., "A Two Equation Turbulence Closure Model for Wall Bounded and Free Shear Flows," AIAA Paper 96-2057, June 1996.

[7]Obremski, H. J., Morkovin, M. V., and Landahl, M., "Portfolio of Stability Characteristics of Incompressible Boundary Layers," AGARDograph 134, March 1969.

[8]Walker, G. J., "Transitional Flow on Axial Turbomachine Blading," *AIAA Journal*, Vol. 27, No. 5, 1989, pp. 595–602.

[9]Dhawan, S., and Narasimha, R., "Some Properties of Boundary Layer Flow During Transition from Laminar to Turbulent Motion," *Journal of Fluid Mechanics*, Vol. 3, No. 4, 1958, pp. 418–436.

[10]Schubauer, G. B., and Klebanoff, P. S., "Contributions on the Mechanics of Boundary-Layer Transition," NACA Rept. 1289, 1956.

[11]Schubauer, G. B., and Skramstad, H. K., "Laminar Boundary Layer Oscillations and Transition on a Flat Plate," NACA Rept. 909, 1948.

[12]Harris, J. E., and Blanchard, D. K., "Computer Program for Solving Laminar, Transitional, or Turbulent Compressible Boundary-Layer Equations for Two-Dimensional and Axisymmetric Flow," NASA TM 83207, Feb. 1982.

[13]Mateer, G. G., Monson, D. J., and Menter, F. R., "Skin-Friction Measurements and Calculations on a Lifting Airfoil," *AIAA Journal*, Vol. 34, No. 2, 1996, pp. 231–236.

[14]Menter, F. R., "Two-Equation Eddy-Viscosity Turbulence Models for Engineering Applications," *AIAA Journal*, Vol. 32, No. 8, 1994, pp. 1598–1605.

A. Plotkin
*Associate Editor*

# Shock Pattern of a Triple-Shock Turbulent Interaction

Datta Gaitonde* and J. S. Shang†
*U.S. Air Force Wright Laboratory,*
*Wright–Patterson Air Force Base, Ohio 45433-7913*

## I. Introduction

AN important factor limiting the performance of supersonic aircraft propulsion systems is the phenomenon of three-dimensional separation that occurs in the compression process. The consequent formation of vortical structures reduces pressure recovery and increases distortion. One of the primary indicators of the flowfield is the shock structure. In a recent work, Garrison et al.[1] present planar laser scattering (PLS) images of the shock structure in the triple-shock (TS) interaction shown schematically in Fig. 1. The incoming equilibrium turbulent boundary layer is subjected to shock waves arising at three compression surfaces, viz., the two 15-deg fins and the 10-deg ramp. The flowfield represents a progression in complexity from a single intersecting wedge corner[2] and the double-fin (DF) configurations, e.g., Ref. 3. Rapid advances in computational technology in the past decade have made possible increasingly sophisticated theoretical studies to model such interactions. It is the objective of this work to computationally investigate the complex shock structure arising in the TS interaction. We validate the computed structure by comparison with the PLS observations of Ref. 1. Subsequently, the computations are employed to map the details of the shock intersections. The flowfield parameters are summarized in Fig. 1. For brevity, the reader is referred to Ref. 4 for computational details. The model is similar to that employed successfully for DF shock structure.[3] Briefly, the three-dimensional Reynolds-averaged equations are solved with a high-resolution upwind-biased scheme and a two-equation $k$–$\epsilon$ turbulence model. The mesh employed consists of $99 \times 107 \times 114$ nodes. A discussion of mesh adequacy can be found in Ref. 4.

## II. Results

The shock structure of TS is highly three dimensional. To facilitate description and comparison with experiment, we employ spanwise cutting planes of the type shown schematically in Fig. 1. Figure 2 depicts the computed results with the magnitude of the three-dimensional pressure gradient $|\nabla p|$ on a sequence of such planes. In each frame, the left, right, and bottom boundaries are the symmetry plane, the right fin, and the ramp surfaces, respectively. The PLS observations may be found in Ref. 1 and are not reproduced here. We note, however, that the comparison with the present calculations is excellent and the modest discrepancies that do exist are noted later. Further, the nomenclature employed (Fig. 2) is identical to that of Ref. 1 with the exception of feature 18 as discussed later.

The shock systems from the left and right fins cross at the symmetry plane. Thus, as the cutting plane is moved downstream, the shock system appears to reflect off the symmetry plane and is described later in this manner. In the subsequent discussion, no temporal significance is attached to terms denoting movement or to the superposed arrows. They refer rather to the apparent motion of the shock trace as the cutting plane is moved downstream. In this context, shocks generally "move" into the upstream fluid and impart it a velocity in the same direction.

Figure 2a shows the structure at a station where the shock systems originating at each ramp-fin corner have not yet "propagated" to the symmetry plane. The features include the inviscid fin shock (1), the corner shock (2), the ramp shock (3), an "embedded" fin

Received Jan. 24, 1997; revision received Aug. 13, 1997; accepted for publication Sept. 24, 1997. This paper is declared a work of the U.S. Government and is not subject to copyright protection in the United States.

*Visiting Scientist, Ohio Aerospace Institute, FIMC, Building 450, Suite 7, 2645 Fifth Street. Senior Member AIAA.

†Senior Scientist, FIMC, Building 450, Suite 7, 2645 Fifth Street. Fellow AIAA.